Am J Physiol Endocrinol Metab
281: E848–E856, 2001.

An integrated ^{2}H and ^{13}C NMR study of gluconeogenesis and TCA cycle flux in humans

JOHN G. JONES,[1] MICHAEL A. SOLOMON,[2] SUZANNE M. COLE,[3]
A. DEAN SHERRY,[1,3] AND CRAIG R. MALLOY[1,2]
[1]*Department of Radiology, University of Texas Southwestern Medical Center, Dallas 75235;* [2]*Department of Internal Medicine, University of Texas Southwestern Medical Center and Department of Veterans Affairs Medical Center, Dallas 75216; and* [3]*Department of Chemistry, University of Dallas, Richardson, Texas 75083*

Received 23 October 2000; accepted in final form 21 May 2001

Jones, John G., Michael A. Solomon, Suzanne M. Cole, A. Dean Sherry, and Craig R. Malloy. An integrated ^{2}H and ^{13}C NMR study of gluconeogenesis and TCA cycle flux in humans. *Am J Physiol Endocrinol Metab* 281: E848–E856, 2001.—Hepatic glucose synthesis from glycogen, glycerol, and the tricarboxylic acid (TCA) cycle was measured in five overnight-fasted subjects by ^{1}H, ^{2}H, and ^{13}C NMR analysis of blood glucose, urinary acetaminophen glucuronide, and urinary phenylacetylglutamine after administration of [1,6-$^{13}C_2$]glucose, $^{2}H_2O$, and [U-$^{13}C_3$]propionate. This combination of tracers allows three separate elements of hepatic glucose production (GP) to be probed simultaneously in a single study: *1*) endogenous GP, *2*) the contribution of glycogen, phospho*enol*pyruvate (PEP), and glycerol to GP, and *3*) flux through PEP carboxykinase, pyruvate recycling, and the TCA cycle. Isotope-dilution measurements of [1,6-$^{13}C_2$] glucose by ^{1}H and ^{13}C NMR indicated that GP in 16-h-fasted humans was 10.7 ± 0.9 $\mu mol \cdot kg^{-1} \cdot min^{-1}$. ^{2}H NMR spectra of monoacetone glucose (derived from plasma glucose) provided the relative ^{2}H enrichment at glucose H-2, H-5, and H-6*S,* which, in turn, reflects the contribution of glycogen, PEP, and glycerol to total GP (5.5 ± 0.7, 4.8 ± 1.0, and 0.4 ± 0.3 $\mu mol \cdot kg^{-1} \cdot min^{-1}$, respectively). Interestingly, ^{13}C NMR isotopomer analysis of phenylacetylglutamine and acetaminophen glucuronide reported different values for PEP carboxykinase flux (68.8 ± 9.8 vs. 37.5 ± 7.9 $\mu mol \cdot kg^{-1} \cdot min^{-1}$), PEP recycling flux (59.1 ± 9.8 vs. 27.8 ± 6.8 $\mu mol \cdot kg^{-1} \cdot min^{-1}$), and TCA cycle flux (10.9 ± 1.4 vs. 5.4 ± 1.4 $\mu mol \cdot kg^{-1} \cdot min^{-1}$). These differences may reflect zonation of propionate metabolism in the liver.

monoacetone glucose; acetaminophen glucuronide; carbon 13; deuterium; gluconeogenesis; liver metabolism

THE LIVER PLAYS A PRINCIPAL ROLE in glucose homeostasis by regulating glucose synthesis and storage in response to the normal changes in daily nutritional and hormonal status. Under postabsorptive conditions, hepatic glycogenolysis and gluconeogenesis contribute to endogenous glucose production (GP) (6, 15–17, 23, 31, 32, 41, 44, 45). Because the majority of gluconeogenic carbons are derived from phospho*enol*pyruvate (PEP) via the tricarboxylic acid (TCA) cycle (1, 6, 23, 31, 32), hepatic GP is also intimately linked to acetyl-CoA oxidation and energy production. Together, these biochemical pathways form a metabolic network (Fig. 1) that is highly responsive to matching the external demand for glucose with the availability of glycogen, gluconeogenic precursors, and energy. Measurements of carbon flux through this network typically combine an isotope dilution measurement of endogenous GP with additional tracer measurements of the contributing pathways (6, 8–10, 15, 18, 18, 25). As one example, GP in fasting humans was determined by analysis of the ^{2}H enrichment at glucose C-6 using the hexamethylenetetramine method and mass spectrometry (MS) after infusion of [6,6-$^{2}H_2$]glucose at a known rate (6). It was possible to also give oral $^{2}H_2O$ and measure the contribution of gluconeogenesis to GP from ^{2}H enrichments at glucose C-5 vs. C-2 after parallel selective degradations of plasma glucose and analysis by MS (6). However, the contributions of glycerol vs. TCA cycle intermediates to gluconeogenesis could not be differentiated in this experiment, nor can ^{13}C tracers be combined with ^{2}H tracers using the hexamethylenetetramine method.

^{13}C tracers have also been used to measure metabolic flux through the network. Endogenous GP was monitored with [U-$^{13}C_6$]glucose by following disappearance of the parent *m+6* isotopomer from plasma glucose (23, 24, 38, 40, 41). Additional metabolic information can be derived from partially labeled glucose molecules generated by recycling of ^{13}C label in this experiment. However, the extent to which the recycled label can be reliably analyzed and related to rates of gluconeogenesis and TCA cycle flux is controversial (24, 26, 28). Others have used tracers, such as [3-^{13}C]lactate, that enter at the level of the TCA cycle along with a separate tracer for measuring endogenous GP (9, 10). Neither [U-$^{13}C_6$]glucose nor [3-^{13}C]lactate tracers, however, can differentiate glucose produced from glycogen, glycerol, or the TCA cycle.

Address for reprint requests and other correspondence: C. R. Malloy, Mary Nell and Ralph B. Rogers Magnetic Resonance Center, 5801 Forest Park Rd., Dallas, TX 75235-9085 (E-mail: craig.malloy@utsouthwestern.edu).

The costs of publication of this article were defrayed in part by the payment of page charges. The article must therefore be hereby marked "*advertisement*" in accordance with 18 U.S.C. Section 1734 solely to indicate this fact.

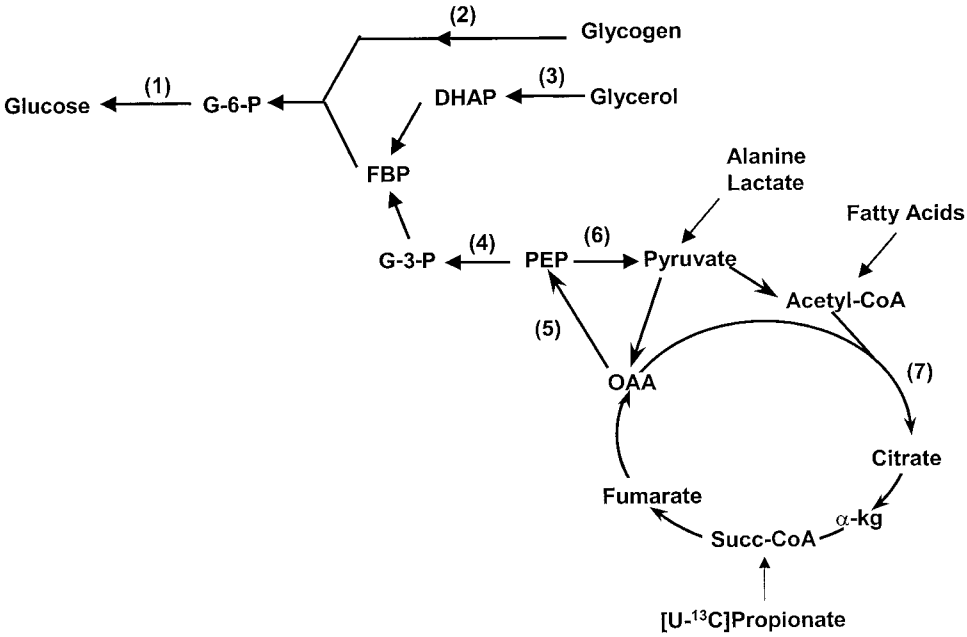

Fig. 1. Metabolic pathways involved in hepatic glucose synthesis and tricarboxylic acid (TCA) cycle activity. G-6-*P*, glucose 6-phosphate; G-3-*P*, glyceraldehyde 3-phosphate; DHAP, dihydroxyacetone phosphate; FBP, fructose bisphosphate; PEP, phospho*enol*pyruvate; OAA, oxaloacetate; Succ-CoA, succinyl-CoA; α-kg, α-ketoglutarate.

In this report, we demonstrate that a ^{2}H NMR spectrum of monoacetone glucose (42) may be used to measure the distribution of deuterium in blood glucose after ingestion of ^2H_2O. This information allows the direct calculation of the contribution of glycogen, glycerol, and the TCA cycle to GP in humans. Although inherently less sensitive, the NMR method offers several advantages over MS analysis of glucose ^{2}H enrichment (31, 32). First, it does not require carbon-by-carbon degradation of glucose; rather, the relative ^{2}H enrichment at each carbon position of glucose can be read out in a single ^{2}H NMR spectrum. Second, the prochiral H-6*R* and H-6*S* resonances are well separated in the ^{2}H NMR spectrum of monoacetone glucose (42); thus the normal assumptions required by MS to quantitatively evaluate exchange at the level of fumarase in the TCA cycle are eliminated. This allows a separate measure of gluconeogenesis from the level of the triose phosphates (glycerol) vs. PEP (the TCA cycle). Finally, the ^{2}H measurement is not compromised by the presence of ^{13}C tracers, so experiments can be designed to measure GP, gluconeogenic flux, pyruvate recycling flux, and TCA cycle flux in a single experiment. We illustrate the method here by reporting these flux values in 16-h-fasted humans using the combined tracers [1,6-$^{13}C_2$]glucose, ^2H_2O, and [U-$^{13}C_3$]propionate. Thus a rather comprehensive picture of liver metabolism can be obtained during a single patient visit, making the technique highly suitable for routine clinical application.

METHODS

Materials. Cambridge Isotopes (Cambridge, MA) was our source for 99% ^2H_2O, 99% [1,6-$^{13}C_2$]glucose, and 99% [U-$^{13}C_3$]propionate. Acetaminophen was derived from regular-strength Tylenol capsules, and phenylacetate was obtained from Sigma (St. Louis, MO).

Experimental protocol. Five healthy, nonobese subjects [2 men and 3 women, 21–36 yr of age, 50–86 (70 ± 14) kg body wt] were studied under a protocol approved by the institutional human studies committee. Subjects were admitted to the General Clinical Research Center at Parkland Hospital and examined (history and physical) by an internist. All had blood glucose levels in the normal range (70–110 mg/dl), and none reported a history of chronic illness or use of medications on a regular basis. All subjects began fasting at 6 PM. At 11 PM and again at 3 AM, 99% ^2H_2O was taken orally (2.5 g/kg body water, calculated as total weight times 0.6 for men or 0.5 for women). During the remainder of the study, 0.5% ^2H_2O was given ad libitum. At 6 AM, subjects ingested a tablet containing 325 mg of acetaminophen. Between 7 and 8 AM, subjects ingested tablets containing phenylacetate (20 mg/kg) and another 650 mg of acetaminophen. At 8 AM, a 3-h primed infusion of [1,6-$^{13}C_2$]glucose (167 mg, 1.67 mg/min) was initiated for each subject. The infusion medium was prepared by dissolving 500 mg of sterile and pyrogen-free [1,6-$^{13}C_2$]glucose into 150 ml of saline. The infusion medium was passed through a 0.22-μm filter during administration. Subjects received a 50-ml bolus of infusion medium over 2 min followed by constant infusion of 30 ml/h. Subjects also ingested [U-$^{13}C_3$]propionate (10 mg/kg, packaged into 3 gel caps) between 8 and 9 AM. Also, beginning at 8 AM, 10 ml of blood were drawn from a contralateral vein every 20 min for 2 h, with additional blood drawn at 2.5 and 3 h. This amounted to seven blood samples and a total of 70 ml of whole blood per subject. Urine was also collected every hour from 8 AM to 2 PM, at which point the study was concluded.

Analytic procedures. For each subject, an aliquot of the [1,6-$^{13}C_2$]glucose infusion medium was frozen and enzymatically assayed for glucose. Blood samples were chilled immediately after being drawn and centrifuged at 4°C in heparinized tubes. The plasma was then processed for ^{13}C and ^{1}H spectroscopy of plasma glucose by perchloric acid extraction, as previously described (21). For ^{2}H NMR analysis of positional deuterium enrichment, two to three plasma extracts from each subject were pooled and lyophilized to complete dryness. Glucose was converted to monoacetone glucose by

use of the method of Landau et al. (31). After lyophilization, the residue containing monoacetone glucose was dissolved in 0.6 ml of 90% acetonitrile-10% ^{2}H-depleted water plus a few grains of sodium bicarbonate (42), and insoluble material was centrifuged and discarded. Urine samples were treated with urease and β-glucuronidase and lyophilized as described previously (21). The extract was then reconstituted in 10 ml of water, and insoluble material was precipitated by centrifugation. The supernatant was adjusted to pH 1.0 with perchloric acid, and the sample was applied to an 8- to 10-ml cation-exchange column (Dowex-50 × 8-H^+) followed by 40 ml of water. The column effluent was neutralized with KOH, lyophilized, and resuspended in 600 μl of ^2H_2O. The pH was then adjusted to 8.0 with NH_4OH, the samples were centrifuged at 13,000 rpm with an Eppendorf centrifuge, and the supernatants were pipetted into 5-mm NMR tubes.

NMR spectroscopy. Proton-decoupled ^{13}C NMR spectra of blood and urine extracts were collected using a Unity Inova 14.1-T spectrometer operating at 150.9 MHz. Free-induction decays were multiplied by a 0.1- to 0.2-Hz exponential function before Fourier transformation. Typically, 9,000–18,000 free-induction decays were summed for each blood extract and 6,000 for each urine extract, resulting in collection times of 5–14 h per extract. Proton-decoupled ^{2}H NMR spectra of monoacetone glucose were acquired at 50°C (42) with the same probe using a 90° pulse and a sweep width of 920 Hz digitized into 992 points, giving an acquisition time of 0.512 s. No additional interpulse delays were used in this pulse sequence. Typically 90,000–100,000 scans were averaged. The data were zero-filled to 4 K, multiplied by a 1-Hz exponential function to increase signal-to-noise ratio, and Fourier transformed. ^{2}H signal intensities obtained with these parameters were corrected for minor effects of differential saturation. A comparison of ^{2}H signal areas in spectra collected using these standard pulsing conditions with those measured in spectra collected using a 1.0-s acquisition time [sufficient for complete relaxation (38)] were identical to within 7%. Nevertheless, small correction factors were used to allow for partial saturation when the 0.512-s acquisition conditions were used. ^{1}H NMR spectra were obtained with the same spectrometer by means of a 5-mm indirect probe. Spectra were acquired with a 90° pulse after presaturation of the residual water signal and a 15-s interpulse delay. Long-range couplings between ^{13}C C-2 to C-6 and H-1α were abolished by the application of a narrow-band WALTZ-16 ^{13}C-decoupling pulse sequence covering the 60- to 75-ppm region of the ^{13}C NMR spectrum (18). Two hundred fifty-six acquisitions were collected for a total collection time of 64 min. All NMR spectra were analyzed using the curve-fitting routine supplied with the NUTS PC-based NMR spectral analysis program (Acorn NMR, Fremont, CA).

Metabolic flux calculations. The ^{13}C enrichment in the [1,6-$^{13}C_2$]glucose used for the infusions was verified by ^{1}H NMR. The fraction of blood glucose that contained ^{13}C in C-1 was defined as *f*, the area of the doublet due to flux (J_{CH}) in the glucose H-1 resonance relative to the total H-1 resonance area (Fig. 2). The fraction of blood glucose that was [1,6-$^{13}C_2$]glucose relative to all glucose containing ^{13}C in C-1 was defined as *g*, the doublet due to flux (J_{CC}) arising from [1,6-$^{13}C_2$]glucose relative to the total area of the glucose C-1 resonance (Fig. 2). The fraction of [1,6-$^{13}C_2$] glucose in plasma glucose was calculated as *fg*. The values measured in spectra collected at 120, 150, and 180 min were averaged for each subject and used in the calculation of GP. The rate of appearance of glucose was calculated from the known infusion rate of [1,6-$^{13}C_2$]glucose (*r*) divided by the average fraction found in plasma over the 120- to 180-min period. GP is then defined as the rate of appearance of glucose minus the rate of infusion of [1,6-$^{13}C_2$]glucose, or GP = (*r*/*fg*) − *r*.

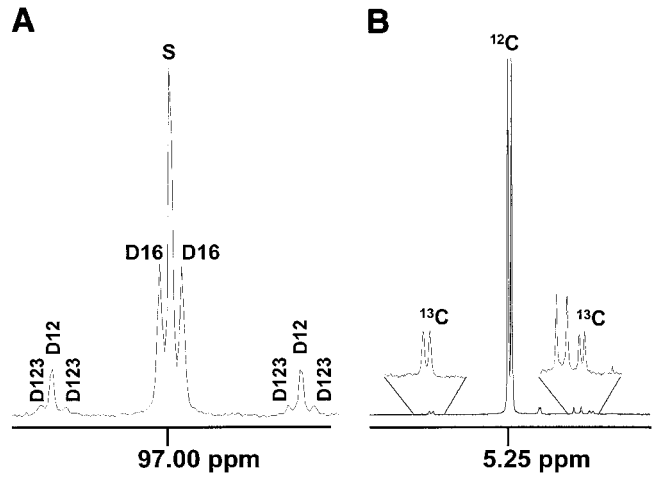

Fig. 2. Plasma glucose C-1β (*A*) and H-1α resonance (*B*) from ^{13}C and ^{1}H NMR spectra of a plasma glucose extract prepared from 10 ml of blood drawn at the end of [1,6-$^{13}C_2$]glucose infusion. S, singlet component; D12, multiplet component from glucose isotopomers with ^{13}C in positions 1 and 2; D123, multiplet component from glucose isotopomers with ^{13}C in positions 1, 2, and 3; D16, multiplet component from glucose isotopomers with ^{13}C in positions 1 and 6.

The fraction of glucose derived from glycogen, PEP, and gluconeogenesis was estimated from the ratio of deuterium enrichment at positions 2, 5, and 6*S* as reported in the ^{2}H NMR spectrum of monoacetone glucose (42) by use of the following equations

$$\text{glucose fraction from glycogen} = 1 - (\text{H-5/H-2}) \quad (1)$$

$$\text{glucose fraction from glycerol} = (\text{H-5} - \text{H-6}S)/\text{H-2} \quad (2)$$

$$\text{glucose fraction from PEP} = \text{H-6}S/\text{H-2} \quad (3)$$

Relative anaplerotic flux (OAA → PEP, where OAA is oxaloacetate), pyruvate recycling flux (PEP → pyruvate or equivalent pathway), and gluconeogenic flux (PEP → glucose) were calculated from the multiplet areas measured in the ^{13}C NMR spectrum of urinary glucuronate or phenylacetylglutamine (PAGN), as described previously (18, 20, 21). For urinary glucuronate C-5 (the C-5β resonance was analyzed), the relevant equations are

$$\text{OAA} \rightarrow \text{PEP} = (\text{C-5D56} - \text{C-5D45})/\text{C-5D45} \quad (4)$$

$$\text{PEP} \rightarrow \text{pyruvate} = (\text{C-5D56} - \text{C-5Q})/\text{C-5D45} \quad (5)$$

$$\text{PEP} \rightarrow \text{glucose} = (\text{C-5Q} - \text{C-5D45})/\text{C-5D45} \quad (6)$$

For PAGN C-2, the relevant equations are

$$\text{OAA} \rightarrow \text{PEP} = (\text{C-2D23} - \text{C-2D12})/\text{C-2D12} \quad (7)$$

$$\text{PEP} \rightarrow \text{pyruvate} = (\text{C-2D23} - \text{C-2Q})/\text{C-2D12} \quad (8)$$

$$\text{PEP} \rightarrow \text{glucose} = (\text{C-2Q} - \text{C-2D12})/\text{C-2D12} \quad (9)$$

Gluconeogenic flux from PEP is the difference between anaplerosis (OAA → PEP) and pyruvate recycling (PEP → pyruvate). PEP recycling is indicated here by PEP → pyruvate, although it should be noted that the combined pathway OAA → PEP → pyruvate cannot be distinguished from malate → pyruvate.

These relative fluxes were then converted to absolute values as follows. First, absolute fluxes in hexose units from

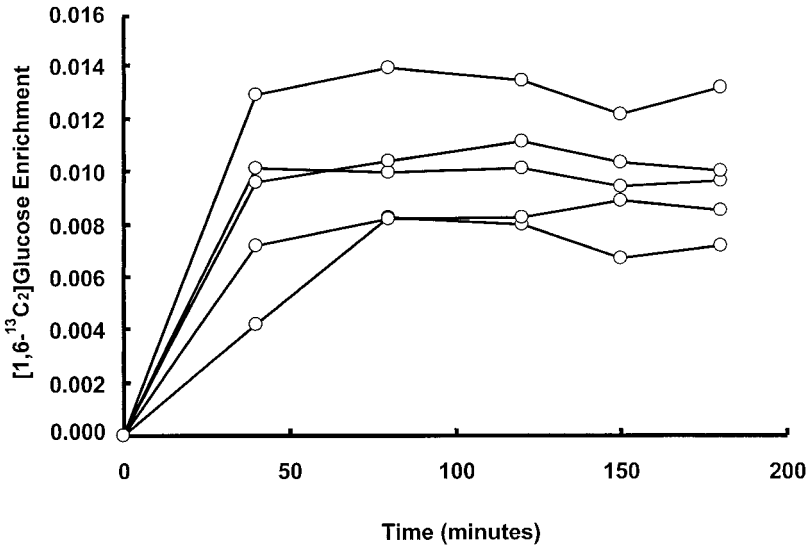

Fig. 3. Time course of plasma [1,6-$^{13}C_2$]glucose enrichment over the duration of [1,6-$^{13}C_2$]glucose infusion for 5 subjects.

glycogen, PEP, and glycerol were defined as the product of each fractional contribution (*Eqs. 1–3*) times the endogenous GP in micromoles of glucose per kilogram per minute. Second, the rate of GP from PEP was converted to the rate of production of PEP by multiplying by 2. Finally, fluxes involved in the TCA cycle were calculated by indexing the relative fluxes (*Eqs. 4–6* or *7–9*) to the rate of production of PEP. For example, if GP is 10 $\mu mol \cdot kg^{-1} \cdot min^{-1}$ and the relative sources of glucose are glycerol (4%), glycogen (50%), and PEP (46%), then the rate of GP from PEP is 4.6 μmol hexose units$\cdot kg^{-1} \cdot min^{-1}$ or 9.2 μmol triose units$\cdot kg^{-1} \cdot min^{-1}$. Flux ratios related to the TCA cycle are defined relative to citrate synthase. Given relative fluxes of OAA $\rightarrow$ PEP (6.5), PEP $\rightarrow$ pyruvate (5), and PEP $\rightarrow$ glucose (1.5), then flux through OAA $\rightarrow$ PEP = 6.5 $\times$ 9.2 $\div$ 1.5 = 39.9 $\mu mol \cdot kg^{-1} \cdot min^{-1}$, and citrate synthase flux = 9.2 $\div$ 1.5 = 6.1 $\mu mol \cdot kg^{-1} \cdot min^{-1}$.

Statistical analysis. Values are means $\pm$ SD. Means were compared as noted using a *t*-test assuming unequal variances.

RESULTS

Each of the three separate components required for analysis of gluconeogenesis is presented individually.

Endogenous GP measurement from [1,6-$^{13}C_2$]glucose. A ^{13}C NMR spectrum of the plasma glucose C-1β resonance from blood taken 180 min after administration of [U-$^{13}C_3$]propionate and [1,6-$^{13}C_2$]glucose is shown in Fig. 2. The resonance features well-resolved multiplets arising from ^{13}C-^{13}C splitting, reflecting the presence of multiply labeled glucose molecules. These include signals from glucose isotopomers generated from the gluconeogenic metabolism of [U-$^{13}C_3$]propionate (D12 and D123) in addition to the tracer amount of infused [1,6-$^{13}C_2$]glucose (D16). As previously demonstrated (18), the fraction of [1,6-$^{13}C_2$]glucose remaining in plasma at any time point can be quantified by measuring the contribution of [1,6-$^{13}C_2$]glucose to the C-1β resonance (^{13}C spectrum) and the total ^{13}C enrichment as reported in the H-1α resonance (^1H spectrum). The ^1H NMR spectrum of the H-1α proton features well-resolved ^{13}C satellites with sufficient signal-to-noise ratio for reliable quantitation of the 2–3% excess ^{13}C enrichment levels from this experiment. Figure 3 summarizes the [1,6-$^{13}C_2$]glucose fractional enrichment values obtained from serial blood sampling for the five subjects. The fractional enrichment of plasma [1,6-$^{13}C_2$]glucose reached steady state well before the end of the infusion, with enrichments of 0.75–1.35%. For each individual, the steady-state enrichment was calculated as the mean of the 120-, 150-, and 180-min enrichments. From these data, average endogenous GP for these five individuals was 10.7 $\pm$ 0.9 $\mu mol \cdot kg^{-1} \cdot min^{-1}$, with a range of 9.8–12.1 $\mu mol \cdot kg^{-1} \cdot min^{-1}$. These values are in good agreement with other measures of endogenous GP in healthy individuals after similar fasting times (the average of all values reported in Refs. 4, 6, 13–15, 23, 27, and 39 is 11.2 $\pm$ 1.7 $\mu mol \cdot kg^{-1} \cdot min^{-1}$).

Analysis of plasma glucose ^2H enrichment by ^2H NMR. Figure 4 shows a ^2H NMR spectrum of monoacetone glucose derived from two pooled plasma extracts (corresponding to 20 ml of whole blood). The area of each resonance is proportional to ^2H enrichment at that position, so the spectrum provides a simple and direct readout of ^2H enrichment ratios (42). It is important to point out that the ^2H NMR measurement is

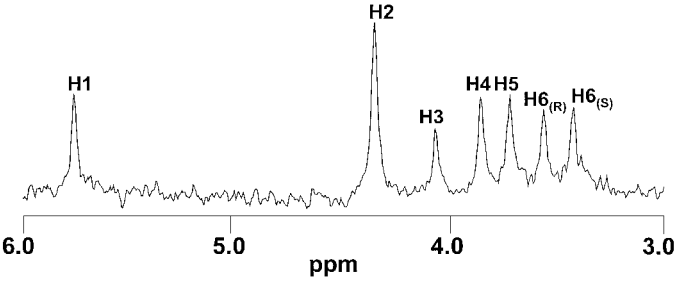

Fig. 4. ^2H NMR spectrum of the 3.0- to 6.0-ppm region featuring the signals of monoacetone glucose that were derived from the 7 aliphatic hydrogens of plasma glucose (H-1 to H-6). The sample was prepared from 2 pooled plasma glucose extracts (60 and 90 min).

Table 1. *Relative fluxes from ^{2}H and ^{13}C NMR analysis*

Subject	Sources of Glucose*			Flux Ratios Relative to Citrate Synthase†			Flux Ratios Relative to Citrate Synthase‡		
	Glycogen (*Eq. 1*)	Glycerol (*Eq. 2*)	PEP (*Eq. 3*)	OAA → PEP (*Eq. 4*)	PEP → pyruvate (*Eq. 5*)	PEP → glucose (*Eq. 6*)	OAA → PEP (*Eq. 7*)	PEP → pyruvate (*Eq. 8*)	PEP → glucose (*Eq. 9*)
AB	0.57	0.00	0.43	6.61	5.18	1.44	6.58	5.90	0.69
JJ	0.55	0.06	0.39	7.41	5.10	2.31	6.34	5.44	0.90
LR	0.43	0.01	0.56	5.50	3.76	1.74	6.15	5.03	1.12
SR	0.45	0.06	0.49	7.51	5.62	1.89	6.80	5.73	1.07
SH	0.59	0.03	0.38	8.53	6.68	1.85	5.66	4.96	0.70
Mean ± SD	0.52 ± 0.07	0.03 ± 0.03	0.45 ± 0.08	7.11 ± 1.13	5.27 ± 1.05	1.85 ± 0.31	6.31 ± 0.44	5.41 ± 0.41	0.90 ± 0.20

Relative contributions of glycogen, glycerol, and phospho*enol*pyruvate (PEP) to blood glucose were measured by ^{2}H NMR of monoacetone glucose derived from blood glucose. Fluxes through key pathways involving the tricarboxylic acid (TCA) cycle were measured relative to flux through citrate synthase by analysis of ^{13}C NMR spectra from urinary acetaminophen glucuronide or urinary phenylacetylglutamine. OAA, oxaloacetate. *Fraction, from ^{2}H NMR of blood monoacetone glucose. †From ^{13}C NMR of urine acetaminophen glucuronide. ‡From ^{13}C NMR of urine phenylacetylglutamine.

not influenced by the presence of tracer levels of ^{13}C in the glucose (or monoacetone glucose) molecule. Table 1 summarizes the relative contributions of glycogen, glycerol, and PEP to GP.

TCA cycle and gluconeogenic flux measurements from [U-$^{13}C_3$]propionate incorporation into hexose and PAGN. As previously demonstrated (21), relative anaplerotic, pyruvate recycling, and gluconeogenic fluxes can be obtained by a ^{13}C isotopomer analysis of plasma glucose, urinary glucuronide, or the glutamine fragment in urinary PAGN. *Equations 4–9* describe these relationships. Figure 5 illustrates typical multiplets observed in the ^{13}C NMR spectrum of plasma glucose C-2β and urinary glucuronate C-5β of the same individual. The multiplet pattern arises from metabolism of [U-$^{13}C_3$]propionate at the level of the liver TCA cycle and is not affected by the presence or metabolism of [1,6-$^{13}C_2$]glucose (18). The difference in signal-to-noise ratio in these two spectra is largely due to the amount of urinary glucuronate in ~100–150 ml of urine compared with the amount of glucose in 10 ml of blood. Given that the multiplets in blood glucose C-2β and urinary glucuronate C-5β report identical flux values (21) and given the large differences in signal-to-noise ratio of the spectra shown, relative flux values as reported by the glucuronate spectra are reported here. Estimates of flux ratios based on acetaminophen glucuronide for five healthy, nonobese individuals were OAA → PEP = 7.1 ± 1.1, PEP → pyruvate = 5.3 ± 1.0, and PEP → glucose = 1.8 ± 0.3 (Table 1).

The ^{13}C NMR spectra of urinary PAGN were also of high quality (Fig. 6). Analysis of the glutamine C-2 multiplets using *Eqs. 7–9* provided the following relative flux estimates (Table 1): OAA → PEP = 6.3 ± 0.4, PEP → pyruvate = 5.4 ± 0.4, and PEP → glucose = 0.9 ± 0.2. As noted in an earlier study of 24- to 28-h-

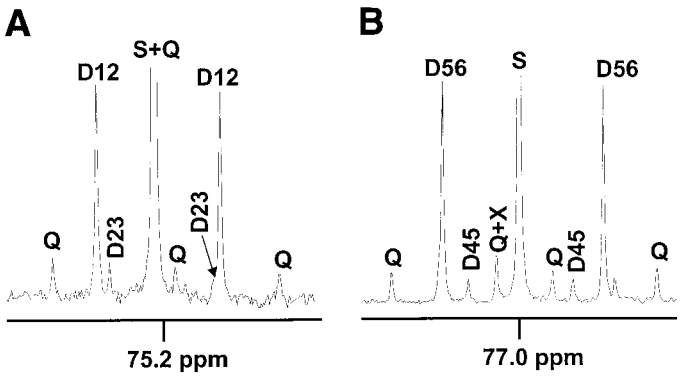

Fig. 5. ^{13}C NMR spectra of the glucose C-2β multiplet from a plasma glucose extract prepared from 10 ml of blood drawn at 150 min after [U-$^{13}C_3$]propionate ingestion (*A*) and the glucuronate C-5β multiplet of a urine extract prepared from urine collected 3–4 h after [U-$^{13}C_3$]propionate ingestion (*B*). Both spectra were obtained from the same subject. S, singlet component; D12, multiplet component from glucose isotopomers with ^{13}C in positions 1 and 2; D23, multiplet component from glucose isotopomers with ^{13}C in positions 2 and 3; Q, multiplet component from glucose isotopomers with ^{13}C in positions 1, 2, and 3 or from glucuronate isotopomers with ^{13}C in positions 4, 5, and 6; D56, multiplet component from glucuronate isotopomers with ^{13}C in positions 5 and 6; D45, multiplet component from glucuronate isotopomers with ^{13}C in positions 4 and 5; X, unknown signal.

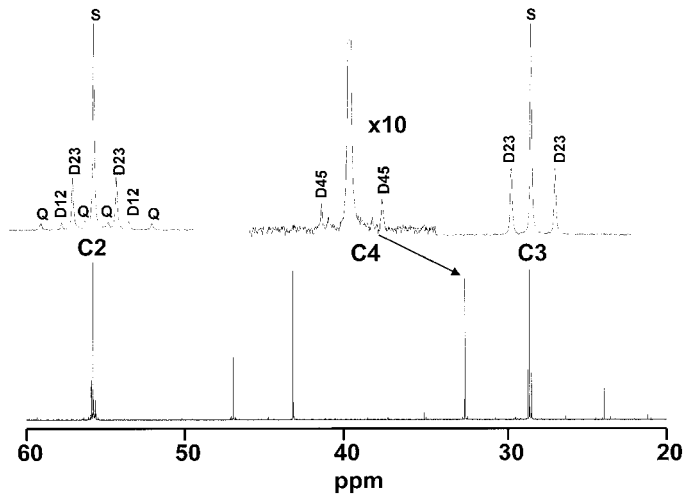

Fig. 6. ^{13}C NMR spectra of phenylacetylglutamine C-2, C-3, and C4 resonances from the 3- to 4-h urine extract. S, singlet component; D12, multiplet component from glutamine isotopomers with ^{13}C in positions 1 and 2; D23, multiplet component from glutamine isotopomers with ^{13}C in positions 2 and 3; D45, multiplet component from glutamine isotopomers with ^{13}C in positions 4 and 5; Q, multiplet component from glutamine isotopomers with ^{13}C in positions 1, 2, and 3.

Table 2. *Fluxes through pathways supporting glucose production*

Subject	Glucose Production, μmol·kg^{-1}·min^{-1} (1)	Rate of Production of Glucose from Each Source, μmol hexose·kg^{-1}·min^{-1}			Fluxes from Analysis of Urine Acetaminophen Glucuronide, μmol·kg^{-1}·min^{-1}			Fluxes from Analysis of Urine, PAGN, μmol·kg^{-1}·min^{-1}		
		Glycogen (2)	Glycerol (3)	PEP (4)	OAA → PEP (5)	PEP → pyruvate (6)	CS (7)	OAA → PEP (5)	PEP → pyruvate (6)	CS (7)
AB	9.8	5.59	0.00	4.21	38.69	30.32	5.85	80.62	72.25	12.25
JJ	10.0	5.50	0.60	3.90	25.02	17.22	3.38	54.90	47.10	8.65
LR	10.7	4.60	0.11	5.99	37.88	25.90	6.89	65.77	53.79	10.70
SR	12.1	5.45	0.73	5.93	47.12	35.26	6.27	75.11	63.25	11.04
SH	11.0	6.49	0.33	4.18	38.55	30.19	4.52	67.54	59.18	11.93
Mean ± SD	10.7 ± 0.9	5.52 ± 0.67	0.35 ± 0.31	4.84 ± 1.03	37.45 ± 7.92	27.78 ± 6.77	5.38 ± 1.42	68.79 ± 9.79	59.11 ± 9.52	10.91 ± 1.41

Results from ^{2}H NMR analysis of blood monoacetone glucose and the measured glucose production were used calculate the rate of glucose production from PEP and other sources. CS, citrate synthase. The rate of production of PEP from the TCA cycle (in triose units) was indexed to flux ratios [calculated from urine acetaminophen glucuronide or urine phenylacetylglutamine (PAGN)] in the TCA cycle to calculate absolute fluxes. Numbers in parentheses refer to the numbered pathways of Fig. 1.

fasted individuals (21), flux estimates determined by analysis of PAGN were significantly different from those derived from spectra of blood glucose or urinary glucuronate. A comparison of the flux ratios derived from acetaminophen glucuronide and PAGN (Table 1) shows a significantly lower relative PEP → glucose flux for PAGN than for glucuronate ($P < 0.01$). There was no significant difference in estimates of PEP → pyruvate or OAA → PEP (relative to citrate synthase, Table 1).

With the methylene carbon of phenylacetate (~44 ppm, 1.1% ^{13}C) as an internal standard, the enrichment in PAGN C-2 and C-3 was 2.13 ± 0.19 and 2.04 ± 0.16%, respectively, while the ^{13}C enrichment in C-4 was essentially equal to natural abundance levels (1.00 ± 0.06%). The enrichment in C-4 reports enrichment in acetyl-CoA and suggests that C-2 of acetyl-CoA was not enriched above natural abundance. However, the PAGN C-4 resonance did show a very small doublet (D45) characteristic of C-4 to C-5 coupling (52 Hz) resulting from entry of [1,2-$^{13}C_2$]acetyl-CoA into the TCA cycle. Because [1,2-$^{13}C_2$]acetyl-CoA can only arise from [1,2,3-$^{13}C_3$]- or [2,3-$^{13}C_2$]pyruvate, the presence of D45 indicates that a small portion of recycled pyruvate was oxidized to acetyl-CoA by pyruvate dehydrogenase. The intensity of the D45 signal was ~5% of that of the C-2 multiplet, indicating that the level of acetyl-CoA labeling was very low compared with that of OAA, pyruvate, and PEP. However, because *Eqs. 4–9* explicitly assume zero labeling of acetyl-CoA (20), this small enrichment of acetyl-CoA could potentially introduce errors into the flux estimates. The possible impact of this on anaplerosis, pyruvate recycling, and gluconeogenic flux estimates was tested by simulating (using tcaSIM[1]) ^{13}C NMR spectra of glutamine for two metabolic situations, one with no labeling of acetyl-CoA and another with entry of 5% [1,2-$^{13}C_2$]acetyl-CoA. Identical flux values (within 5%) were obtained by analysis of the resulting glutamate C-2 multiplet areas with the use of *Eqs. 7–9*. We conclude that enrichment of glutamate C-4 at the level seen here in PAGN does not interfere with accurate measurement of the metabolic fluxes of interest.

Integration of metabolic data. The relative flux values reported by the [U-$^{13}C_3$]propionate and ^2H_2O tracers were converted to absolute flux values by referencing them to GP as reported by turnover of [1,6-$^{13}C_2$] glucose. This provides the rather comprehensive picture of TCA cycle-related fluxes and gluconeogenesis summarized in Table 2. Absolute flux estimates are reported for glucuronate- and PAGN-based ^{13}C-isotopomer analyses.

DISCUSSION

This study demonstrates that a comprehensive metabolic profile of gluconeogenesis and TCA cycle activity may be obtained in humans with three stable isotope tracers and NMR analysis of blood and urine samples. Multiple tracers were required, because multiple experimental determinations are necessary to describe the known pathways involved in gluconeogenesis. These data were obtained after enrichment of total body water with ^2H_2O and two ^{13}C tracers, [1,6-$^{13}C_2$] glucose to measure endogenous GP and [U-$^{13}C_3$] propionate as an index of TCA cycle activity.

^{2}H NMR of monoacetone glucose. The ^{2}H NMR spectrum of monoacetone glucose (42) derived from 20 ml of plasma glucose provided a convenient, direct measure of ^{2}H enrichment at each site in the glucose molecule. Enrichment at H-2, reflecting isotopic equilibration of plasma glucose H-2 with body water (4, 8, 39), was highest in every sample, while enrichment at H-5 was ~50% of that at H-2. This indicates that glycogenolysis and gluconeogenesis contribute equally to endogenous GP after a 16- to 18-h fast. These observations agree with gas chromatography (GC)-MS measurements of H-5 and H-2 enrichments in 14- and 18.5-h-fasted individuals, where the contribution of gluconeogenesis to endogenous GP was reported to be 47 ± 4 and 54 ±

[1]tcaSIM is an isotopomer simulation program; it is available by e-mail (mark.jeffrey@utsouthwestern.edu), or it can be downloaded from the "Available Products" page of the Rogers Center website (www2.swmed.edu/rogersmr2). Address requests by mail to F. M. H. Jeffrey, Mary Nell and Ralph B. Rogers Center, 5801 Forest Park Rd., Dallas, TX 75235-9085.

2%, respectively (6, 31). Furthermore, the observation that ^{2}H enrichment at H-6*S* was ~95% of that at H-5 indicates that the majority of gluconeogenic carbons are derived from the TCA cycle (PEP) and very few from glycerol (4, 8, 31). Most importantly, the ^{2}H NMR spectrum of monoacetone glucose shows separate resonances for the prochiral H-6 hydrogens of glucose (42), while exchange of ^2H_2O at the level of fumarase in the TCA cycle specifically enriches the H-6*S* position (46). Interestingly, the prochiral H-6 protons had comparable levels of enrichment, with a tendency toward higher enrichment in H-6*S*.

The capacity to measure individual enrichment of the prochiral glucose hydrogens by ^{2}H NMR provides additional insight into the mechanisms that contribute to the enrichment of the methylene hydrogens of PEP from body water. Although the exchange mechanisms for enriching H-2 and H-5 of glucose from body water are considered to be essentially quantitative, exchange of pyruvate and water hydrogens is believed to be only 80% complete (31). If this is true, then enrichment of the PEP methylene hydrogens would be less than that of body water, and the H-6-to-H-2 enrichment ratio of glucose as measured by GC-MS would underestimate the contribution of PEP to GP. However, this should only be true for glucose H-6*R,* because pyruvate enrichment is reported by the pro-*S* hydrogen of OAA[2], while the pro-*R* hydrogen of this intermediate can undergo complete exchange with body water by interconversion with malate and fumarate (Fig. 7). If randomization between OAA, malate, and fumarate is complete, then ^{2}H enrichment at the pro-*R* hydrogen of OAA would equal that of body water. Thus, to the extent that randomization is incomplete, enrichment of the pro-*R* hydrogen of OAA will be a weighted average of pyruvate and body water enrichments. However, given that carbon tracer data from this and other studies have demonstrated that there is extensive backward scrambling of OAA with fumarate as well as extensive recycling of PEP, pyruvate, and OAA in liver (9, 10, 19, 32), it is perhaps not surprising to find that glucose H-6*R* and H-6*S* had near-equivalent levels of ^{2}H enrichment from ^2H_2O. This observation means that the H-6-to-H-2 enrichment ratio reported by GC-MS (a single H-6 measurement is taken, and a ^{2}H enrichment distributed equally between H-6*R* and H-6*S* is assumed) should be equivalent to the H-6*S*-to-H-2 ratio reported by ^{2}H NMR.

TCA cycle fluxes. In this study, PEP carboxykinase and pyruvate recycling fluxes were about seven- and fivefold higher than TCA cycle flux, while net gluconeogenic outflow (defined as PEP → glucose flux) was about twofold greater than TCA cycle flux. Compared with 24- to 28-h-fasted individuals (19), gluconeogenic outflow in the present group (fasted for 16–18 h) tended to be lower, while PEP carboxykinase and pyruvate recycling fluxes tended to be higher.

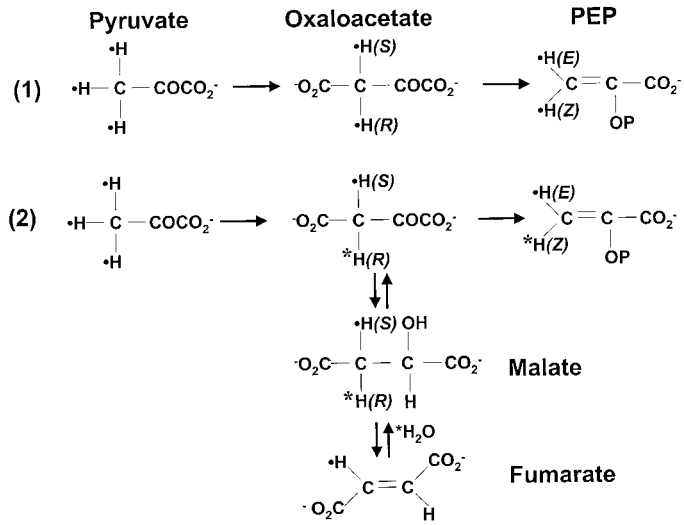

Fig. 7. Labeling of the prochiral methylene hydrogens of PEP from pyruvate and body water in the absence (*1*) and presence (*2*) of exchange between OAA, malate, and fumarate. ∗, Labeled hydrogen derived from labeled water as a result of fumarase activity. ●, labeled hydrogen derived from pyruvate.

Estimates of relative PEP → glucose flux show a large variation between different studies. In the study of Magnusson et al. (35), PEP → glucose flux was approximately three times citrate synthase flux for 60-h-fasted individuals and overnight-fasted subjects given intravenous glucose and glucagon. In comparison, the values reported by Diraison et al. (9, 10) are only ~0.5 times flux through citrate synthase. Absolute TCA cycle fluxes are derived by indexing relative fluxes to an independent measurement of absolute PEP → glucose flux; therefore, uncertainties in relative PEP → glucose flux propagate systematic uncertainties in estimates of absolute TCA cycle fluxes. For example, absolute hepatic citrate synthase fluxes estimated by Diraison et al. range from 20 to 35 $\mu mol \cdot kg^{-1} \cdot min^{-1}$, while estimates[3] from Magnusson et al. range from 5 to 7 $\mu mol \cdot kg^{-1} \cdot min^{-1}$. Absolute citrate synthase flux estimates from our study (5.4 and 10.9 $\mu mol \cdot kg^{-1} \cdot min^{-1}$ from urinary glucuronate and PAGN, respectively) are similar to the estimates of Magnusson et al. No other published estimates of human hepatic citrate synthase flux are available for comparison.

The anaplerotic, PEP recycling, and TCA cycle fluxes reported here are based on a simple set of equations that are valid when excess enrichment of acetyl-CoA and C-4 and C-5 of PAGN are negligible relative to enrichment of C-1 to C-3 (18). The advantage of such equations over computational analysis is that they provide a simple and direct way of relating the C-2 multiplet pattern from the ^{13}C NMR spectrum of glucose or PAGN to metabolic fluxes through anaplerotic,

[2] *R*-[3-^{2}H]OAA → (*Z*)-[3-^{2}H]PEP → *S*-[3-^{2}H]PEP → → *S*-[6-^{2}H]glucose; *S*-[3-^{2}H]OAA → (*E*)-[3-^{2}H]PEP → *R*-[3-^{2}H]PEP → → *R*-[6-^{2}H]-glucose (46).

[3] Published flux estimates in millimoles per minute were converted to micromoles per kilogram per minute using the reported average weight of the subjects.

recycling, and oxidative pathways (16, 18, 19). Although the relative enrichments of PAGN C-4 encountered in the present study were sufficiently low for the simple equations to be valid, there may be circumstances where the relative enrichment of C-4 is high enough to introduce significant errors into metabolic flux estimates derived by this method. For example, in 60-h-fasted subjects infused with [3-^{14}C]lactate, the specific activity of C-4 relative to C-2 and C-3 of PAGN was substantially higher than that in subjects infused with [2-^{14}C]propionate or [3-^{14}C]propionate (27). In overnight-fasted subjects infused with [3-^{13}C]lactate, excess enrichment in C-4 of PAGN was 35–42% of that in C-2 and C-3 (9, 10). On the basis of these results, it is likely that a [U-$^{13}C_3$]lactate tracer might also generate more enriched acetyl-CoA and a higher relative enrichment of PAGN C-4 than [U-$^{13}C_3$]propionate under the same physiological conditions. Such conditions generate more complex isotopomer distributions and require computational analysis for obtaining metabolic flux estimates (12, 34). The labeling discrepancies between propionate and lactate tracers likely reflect heterogeneous metabolism of these substrates within the hepatic lobule. Given that propionate is quantitatively extracted from the portal circulation while lactate is not, it is probable that most of the propionate tracer is metabolized by the highly gluconeogenic periportal cells. Consequently, the perivenous cells are exposed to little [U-$^{13}C_3$]propionate tracer directly but are likely to encounter secondary labeled products of periportal [U-$^{13}C_3$]propionate metabolism, such as ^{13}C-enriched glucose or lactate. We hypothesize that this mechanism could contribute to the different isotopomer distributions of the OAA moieties of hepatic glucose and glutamine from [U-$^{13}C_3$]propionate (19). In comparison, a lactate tracer is likely to be more evenly distributed across the lobule; hence, the labeling pattern may reflect a different combination of periportal and perivenous metabolism, resulting in analyte labeling distributions that are different from those obtained from a propionate tracer. The question of which tracer and analyte combination best describes human hepatic TCA cycle activity remains outstanding and will require correlation of metabolic flux estimates with measurements of hepatic arteriovenous substrate balances and glycogen levels.

Analytic considerations. A minimum of 20 ml of whole blood was required for the ^{2}H NMR measurements of plasma glucose under conditions where total body water is enriched to ~0.5% in ^{2}H. Although this amount of blood can be safely collected from adults, this volume would be excessive for small children. Thus, for an equivalent study in children, one would be required to increase the NMR sensitivity by using smaller-volume ^{2}H microprobes, or perhaps cryoprobes, or by collecting larger amounts of glucose equivalents via urinary glucuronide (31). Although ~1.0 mmol of glucuronide might be available in urine (compared with ~0.11 mmol from 20 ml of blood), this must be weighed against the loss of ^{2}H data from the H-6 position (glucose C-6 becomes a carboxylate in the glucuronide) and the additional synthetic steps involved in the conversion of acetaminophen glucuronide to monoacetone glucose. Clearly, the preference would be to perform the ^{2}H analysis on plasma glucose whenever possible.

In summary, any comprehensive analysis of gluconeogenesis in humans requires multiple tracers. Existing protocols typically require experimental studies at different times to account for the complex pathways involving the TCA cycle. The combined ^{2}H-^{13}C NMR isotopomer method reported here allows a practical clinical method for measuring gluconeogenesis in a single study. Furthermore, all the experimental data are collected from blood or urine, and placing humans into magnets is not required. Given that the metabolic tracers can be administered orally and that all data can potentially be collected from urinary metabolites, this method now offers, for the first time, the possibility of a noninvasive examination for outpatient studies that may prove valuable in population-based studies of glucose metabolism.

We acknowledge the excellent technical assistance and support provided by the staff of the General Clinical Research Center at the University of Texas Southwestern Medical Center.

This research was supported by National Institutes of Health Grants RR-02584, HL-34557, and M01-RR-00633.

REFERENCES

1. **Baba H, Zhang XJ, and Wolfe RR.** Glycerol gluconeogenesis in fasting humans. *Nutrition* 11: 149–153, 1995.
2. **Beylot M, Peroni O, Diraison F, and Large V.** New methods for in vivo studies of hepatic metabolism. *Reprod Nutr Dev* 36: 363–373, 1996.
3. **Beylot M, Peroni O, Diraison F, and Large V.** In vivo studies of intrahepatic metabolic pathways. *Diabetes Metab* 23: 251–257, 1997.
4. **Bugianesi E, Kalhan SC, Burkett E, Marchesini G, and McCullough A.** Quantification of gluconeogenesis in cirrhosis: response to glucagon. *Gastroenterology* 115: 1530–1540, 1998.
5. **Burgess S, Jones JG, Sherry AD, and Malloy CR.** Analysis of plasma glucose ^{2}H and ^{13}C labeling following administration of ^{2}H and ^{13}C gluconeogenic tracers (Abstract no. 221). *Experimental NMR Conference 41st Meeting, 2000*.
6. **Chandramouli V, Ekberg K, Schumann WC, Kalhan SC, Wahren J, and Landau BR.** Quantifying gluconeogenesis during fasting. *Am J Physiol Endocrinol Metab* 273: E1209–E1215, 1997.
7. **Chandramouli V, Ekberg K, Schumann WC, Wahren J, and Landau BR.** Origins of the hydrogen bound to carbon 1 of glucose in fasting: significance in gluconeogenesis quantitation. *Am J Physiol Endocrinol Metab* 277: E717–E723, 1999.
8. **Chen X, Iobal N, and Boden G.** The effects of free fatty acids on gluconeogenesis and glycogenolysis in normal subjects. *J Clin Invest* 103: 365–372, 1999.
9. **Diraison F, Large V, Brunengraber H, and Beylot M.** Noninvasive tracing of liver intermediary metabolism in normal subjects and in moderately hyperglycaemic NIDDM subjects. Evidence against increased gluconeogenesis and hepatic fatty acid oxidation in NIDDM. *Diabetologia* 41: 212–220, 1998.
10. **Diraison F, Large V, Maugeais C, Krempf M, and Beylot M.** Noninvasive tracing of human liver metabolism: comparison of phenylacetate and apoB-100 to sample glutamine. *Am J Physiol Endocrinol Metab* 277: E529–E536, 1999.
11. **Ekberg K, Chandramouli V, Kumaran K, Schumann WC, Wahren J, and Landau BR.** Gluconeogenesis and glucuronidation in liver in vivo and the heterogeneity of hepatocyte function. *J Biol Chem* 270: 21715–21717, 1995.

12. **Fernandez CA and Des Rosiers C.** Modeling of liver citric acid cycle and gluconeogenesis based on ^{13}C mass isotopomer distribution analysis of intermediates. *J Biol Chem* 270: 10037–10042, 1995.
13. **Ferrannini E, Bjorkman O, Reichard GA Jr, Pilo A, Olsson M, Wahren J, and DeFronzo RA.** The disposal of an oral glucose load in healthy subjects. A quantitative study. *Diabetes* 34: 580–588, 1985.
14. **Ferrannini E, Simonson DC, Katz LD, Reichard G Jr, Bevilacqua S, Barrett EJ, Olsson M, and DeFronzo RA.** The disposal of an oral glucose load in patients with non-insulin-dependent diabetes. *Metab Clin Exp* 37: 79–85, 1988.
15. **Hellerstein MK, Neese RA, Linfoot P, Christiansen M, Turner S, and Letscher A.** Hepatic gluconeogenic fluxes and glycogen turnover during fasting in humans. A stable isotope study. *J Clin Invest* 100: 1305–1319, 1997.
16. **Hellerstein MK, Neese RA, Schwartz JM, Turner S, Faix D, and Wu K.** Altered fluxes responsible for reduced hepatic glucose production and gluconeogenesis by exogenous glucose in rats. *Am J Physiol Endocrinol Metab* 272: E163–E172, 1997.
17. **Hwang JH, Perseghin G, Rothman DL, Cline GW, Magnusson I, Petersen KF, and Shulman GI.** Impaired net hepatic glycogen synthesis in insulin-dependent diabetic subjects during mixed meal ingestion. A ^{13}C nuclear magnetic resonance spectroscopy study. *J Clin Invest* 95: 783–787, 1995.
18. **Jones JG, Carvalho RA, Franco B, Sherry AD, and Malloy CR.** Measurement of hepatic glucose output, Krebs cycle, and gluconeogenic fluxes by NMR analysis of a single plasma glucose sample. *Anal Biochem* 263: 39–45, 1998.
19. **Jones JG, Carvalho RA, Sherry AD, and Malloy CR.** Quantitation of gluconeogenesis by ^{2}H nuclear magnetic resonance analysis of plasma glucose following ingestion of $^{2}H_2O$. *Anal Biochem* 277: 121–126, 2000.
20. **Jones JG, Naidoo R, Sherry AD, Jeffrey FMH, Cottam GL, and Malloy CR.** Measurement of gluconeogenesis and pyruvate recycling in the rat liver: a simple analysis of glucose and glutamate isotopomers during metabolism of [1,2,3-$^{13}C_3$] propionate. *FEBS Lett* 412: 131–137, 1997.
21. **Jones JG, Solomon MA, Sherry AD, Jeffrey FMH, and Malloy CR.** ^{13}C NMR measurements of human gluconeogenic fluxes after ingestion of [U-$^{13}C_3$]propionate, phenylacetate, and acetaminophen. *Am J Physiol Endocrinol Metab* 275: E843–E852, 1998.
22. **Katz J and Rognstad R.** The metabolism of tritiated glucose by rat adipose tissue. *J Biol Chem* 241: 3600–3610, 1966.
23. **Katz J and Tayek JA.** Gluconeogenesis and the Cori cycle in 12-, 20-, and 40-h-fasted humans. *Am J Physiol Endocrinol Metab* 275: E537–E542, 1998.
24. **Katz J and Tayek JA.** Recycling of glucose and determination of the Cori cycle and gluconeogenesis. *Am J Physiol Endocrinol Metab* 277: E401–E407, 1999.
25. **Katz J, Wals P, and Lee WNP.** Isotopomer studies of gluconeogenesis and the Krebs cycle with ^{13}C-labeled lactate. *J Biol Chem* 268: 25509–25521, 1993.
26. **Kelleher JK.** Estimating gluconeogenesis with [U-$^{13}C_6$]glucose: molecular condensation requires a molecular approach. *Am J Physiol Endocrinol Metab* 277: E395–E400, 1999.
27. **Kruszynska YT, Meyer-Alber A, Darakhshan F, Home PD, and McIntyre N.** Metabolic handling of orally administered glucose in cirrhosis. *J Clin Invest* 91: 1057–1066, 1993.
28. **Landau BR.** Limitations in the use of [U-$^{13}C_6$]glucose to estimate gluconeogenesis. *Am J Physiol Endocrinol Metab* 277: E408–E413, 1999.
29. **Landau BR, Chandramouli V, Schumann WC, Ekberg K, Kumaran K, Kalhan SC, and Wahren J.** Estimates of Krebs cycle activity and contributions of gluconeogenesis to hepatic glucose production in fasting healthy subjects and IDDM patients. *Diabetologia* 38: 831–838, 1995.
30. **Landau BR, Schumann WC, Chandramouli V, Magnusson I, Kumaran K, and Wahren J.** ^{14}C-labeled propionate metabolism in vivo and estimates of hepatic gluconeogenesis relative to Krebs cycle flux. *Am J Physiol Endocrinol Metab* 265: E636–E647, 1993.
31. **Landau BR, Wahren J, Chandramouli V, Schumann WC, Ekberg K, and Kalhan SC.** Use of $^{2}H_2O$ for estimating rates of gluconeogenesis: application to the fasted state. *J Clin Invest* 95: 172–178, 1995.
32. **Landau BR, Wahren J, Chandramouli V, Schumann WC, Ekberg K, and Kalhan SC.** Contributions of gluconeogenesis to glucose production in the fasted state. *J Clin Invest* 98: 378–385, 1996.
33. **Landau BR, Wahren J, Previs SF, Ekberg K, Chandramouli V, and Brunengraber H.** Glycerol production and utilization in humans: sites and quantitation. *Am J Physiol Endocrinol Metab* 271: E1110–E1117, 1996.
34. **Magnusson I, Chandramouli V, Schumann WC, Kumaran K, Wahren J, and Landau BR.** Pentose pathway in human liver. *Proc Natl Acad Sci USA* 85: 4682–4685, 1988.
35. **Magnusson I, Schumann WC, Bartsch GE, Chandramouli V, Kumaran K, Wahren J, and Landau BR.** Noninvasive tracing of Krebs cycle metabolism in liver. *J Biol Chem* 266: 6975–6984, 1991.
36. **Malaisse W, Ladriere JL, Verbruggen I, Grue-Sorenson G, Bjorkling F, and Willem R.** Metabolism of [1,3-^{13}C]glycerol-1,2,3-tris(methylsuccinate) and glycerol-1,2,3-tris(methyl[2,3-^{13}C] succinate) in rat hepatocytes. *Metabolism* 49: 178–185, 2000.
37. **Malloy CR, Sherry AD, and Jeffrey FMH.** Evaluation of carbon flux and substrate selection through alternate pathways involving the citric acid cycle of the heart by ^{13}C NMR spectroscopy. *J Biol Chem* 263: 6964–6971, 1988.
38. **Peroni O, Large V, Diraison F, and Beylot M.** Glucose production and gluconeogenesis in postabsorptive and starved normal and streptozotocin-diabetic rats. *Metabolism* 46: 1358–1363, 1997.
39. **Petersen KF, Krssak M, Navarro V, Chandramouli V, Hundal R, Schumann W, Landau BR, and Shulman GI.** Contribution of net hepatic glycogenolysis and gluconeogenesis to glucose production in cirrhosis. *Am J Physiol Endocrinol Metab* 276: E529–E535, 1999.
40. **Rognstad R, Clark G, and Katz J.** Glucose synthesis in tritiated water. *Eur J Biochem* 47: 383–388, 1974.
41. **Rothman DL, Magnusson I, Katz LD, Shulman RG, and Shulman GI.** Quantitation of hepatic glycogenolysis and gluconeogenesis in fasting humans with ^{13}C NMR. *Science* 254: 573–576, 1991.
42. **Schleucher J, Vanderveer PJ, and Sharkey TD.** Export of carbon from chloroplasts at night. *Plant Physiol* 118: 1439–1445, 1998.
43. **Suvunrungsi L, Jones JG, Sherry AD, Cao L, and Malloy CR.** Comparison of [U-$^{13}C_3$]propionate and [U-$^{13}C_3$]alanine as tracers of hepatic gluconeogenesis and Krebs cycle fluxes (Abstract). *ISMRM 11th Meeting, 2000,* p. 1009.
44. **Tayek JA and Katz J.** Glucose production, recycling, and gluconeogenesis in normals and diabetics: a mass isotopomer [U-$^{13}C_6$]glucose study. *Am J Physiol Endocrinol Metab* 270: E709–E717, 1996.
45. **Tayek JA and Katz J.** Glucose production, recycling, Cori cycle, and gluconeogenesis in humans: relationship to serum cortisol. *Am J Physiol Endocrinol Metab* 272: E476–E484, 1997.
46. **Walsh C.** *Enzymatic Reaction Mechanisms.* New York: Freeman, 1979, p 535–536, 709–711.
47. **Wykes LJ, Jahoor F, and Reeds PJ.** Gluconeogenesis measured with [U-$^{13}C_6$]glucose and mass isotopomer analysis of apoB-100 amino acids in pigs. *Am J Physiol Endocrinol Metab* 274: E365–E376, 1998.